

Extracting $B \rightarrow K^*$ Form Factors from Data

Christian Hambrock* and Gudrun Hiller†

Institut für Physik, Technische Universität Dortmund, D-44221 Dortmund, Germany

We extract ratios of $B \rightarrow K^*$ form factors at low hadronic recoil from recent data on $B \rightarrow K^* \mu^+ \mu^-$ decays in a model-independent way. The presented method will improve in the future with further (angular) studies in semileptonic rare B -decays and advance our understanding of form factors, which are important inputs in precision tests of the Standard Model.

Introduction. The experimental studies of flavor changing neutral current (FCNCs) decays of b -flavored hadrons are advancing rapidly with the successful start of the Large Hadron Colliders' (LHC) b -physics program. This generates further demand for good control of hadronic uncertainties to enable precision tests of the Standard Model (SM).

A leading source of theoretical uncertainty in semileptonic FCNC decays $B \rightarrow M \bar{\ell} \ell$, $\ell = e, \mu, \tau, \nu$ of a B meson into a light meson M are the transition form factors. When the energy of the emitted meson is large in the B meson rest frame, the method of light cone QCD sum rules (LCSR) applies and allows to calculate the form factors in this kinematical regime [1]. The region in which the emitted meson is softly recoiling against the decaying B meson is accessible to lattice QCD. Preliminary unquenched results are available [2]. As we rely on such predictions to probe electroweak and flavor physics, it is important to obtain further independent information.

The low recoil region allows for observables in which the form factors can be probed model-independently [3]. Two of these short-distance free observables, the fraction of longitudinally polarized vector mesons F_L and the transverse asymmetry $A_T^{(2)}$ [4], have recently been measured by CDF [5], BaBar [6] (F_L only) and LHCb [7] in the decay $B \rightarrow K^* \mu^+ \mu^-$. Here, we extract ratios of $B \rightarrow K^*$ form factors from these data. Since the ratios are obtained at low recoil they can be directly compared to lattice predictions. It is the aim of this letter to demonstrate the performance of this new model-independent method from the first time available precision data.

$B \rightarrow K^* \ell^+ \ell^-$ at low recoil. The transversity amplitudes $A_{\perp, ||, 0}^{L, R}$ in $B \rightarrow K^* \ell^+ \ell^-$ decays at low recoil factorize at lowest order [8] and share universal short-distance coefficients $C^{L, R}$ [3]

$$A_i^{L, R} \propto C^{L, R} f_i, \quad i = \perp, ||, 0, \quad (1)$$

while the form factors f_i are independent of the Wilson coefficients of the electroweak theory. A fourth transversity amplitude arises for finite lepton mass m_ℓ . However, at low recoil it is suppressed by m_ℓ^2/m_B^2 , where m_B denotes mass of the B -meson, and can be safely neglected. (We suppress the dependence on the dilepton invariant mass squared q^2 for brevity in this work.)

It follows that observables of type $(A_i^L A_j^{L*} \pm A_i^R A_j^{R*})/(A_l^L A_k^{L*} \pm A_l^R A_k^{R*})$, where $i, j, k, l = \perp, ||, 0$, probe long-distance physics only. This includes F_L and $A_T^{(2)}$, given as [4]

$$F_L = \frac{|A_0^L|^2 + |A_0^R|^2}{\sum_{X=L, R} (|A_0^X|^2 + |A_\perp^X|^2 + |A_{||}^X|^2)}, \quad (2)$$

$$A_T^{(2)} = \frac{|A_\perp^L|^2 + |A_\perp^R|^2 - |A_{||}^L|^2 - |A_{||}^R|^2}{|A_\perp^L|^2 + |A_\perp^R|^2 + |A_{||}^L|^2 + |A_{||}^R|^2}. \quad (3)$$

Using Eq. (1) one obtains at fixed q^2 [3],

$$F_L = \frac{f_0^2}{f_0^2 + f_\perp^2 + f_{||}^2}, \quad A_T^{(2)} = \frac{f_\perp^2 - f_{||}^2}{f_\perp^2 + f_{||}^2}. \quad (4)$$

The f_i read

$$f_\perp = \mathcal{N} \frac{\sqrt{2\hat{s}\hat{\lambda}}}{1 + \hat{m}_{K^*}} V, \quad f_{||} = \mathcal{N} \sqrt{2\hat{s}} (1 + \hat{m}_{K^*}) A_1, \\ f_0 = \mathcal{N} \frac{(1 - \hat{s} - \hat{m}_{K^*}^2)(1 + \hat{m}_{K^*})^2 A_1 - \hat{\lambda} A_2}{2 \hat{m}_{K^*} (1 + \hat{m}_{K^*})}, \quad (5)$$

with

$$\mathcal{N} = G_F \alpha_e V_{tb} V_{ts}^* \sqrt{\frac{m_B^3 \sqrt{\hat{\lambda}}}{3 \times 2^{10} \pi^5}}, \quad \hat{s} = \frac{q^2}{m_B^2}, \quad \hat{m}_{K^*} = \frac{m_{K^*}}{m_B}, \\ \hat{\lambda} = 1 + \hat{s}^2 + \hat{m}_{K^*}^4 - 2(\hat{s} + \hat{s} \hat{m}_{K^*}^2 + \hat{m}_{K^*}^2). \quad (6)$$

The relevant $B \rightarrow K^*$ q^2 -dependent form factors V, A_1 and A_2 are defined as usual [9]:

$$\langle K^*(k, \epsilon) | \bar{s} \gamma_\mu b | B(p) \rangle = \frac{2V}{m_B + m_{K^*}} \epsilon_{\mu\rho\sigma\tau} \epsilon^{\rho\sigma} p^\sigma k^\tau, \quad (7)$$

$$\langle K^*(k, \epsilon) | \bar{s} \gamma_\mu \gamma_5 b | B(p) \rangle = \\ i\epsilon^{\rho\sigma} \left[2A_0 m_{K^*} \frac{q_\mu q_\rho}{q^2} + A_1 (m_B + m_{K^*}) (g_{\mu\rho} - \frac{q_\mu q_\rho}{q^2}) \right. \\ \left. - A_2 q_\rho \left(\frac{(p+k)_\mu}{m_B + m_{K^*}} - \frac{m_B - m_{K^*}}{q^2} (p-k)_\mu \right) \right], \quad (8)$$

where ϵ denotes the polarization vector of the K^* .

It is clear from Eqs. (4) and (5), that one can obtain ratios of form factors V/A_1 and A_1/A_2 by resorting to the observables F_L and $A_T^{(2)}$. We comment on

the limitations of this determination: The universality of Eq. (1) is broken by power corrections at order $1/m_b$ to the improved Isgur-Wise form factor relations between the form factors of the dipole currents $T_{1,2,3}$ [9] and the form factors of the axial and axial-vector currents. However, these corrections enter the transversity amplitudes with additional parametric suppression by the Wilson coefficients C_j of the $|\Delta B| = |\Delta S| = 1$ effective Hamiltonian $C_7/C_9 \sim \mathcal{O}(0.1)$ [3, 8]. Hence, we expect corrections at most at the level of a few percent, as for the $1/m_b$ -corrections to the operator product expansion (OPE) [10]. Further corrections to Eq. (1) arise in extensions of the SM with right-handed currents, which induce a finite $A_T^{(2)}$ at low q^2 . On the other hand, if SM-like chiralities are present only, $A_T^{(2)}$ vanishes up to tiny corrections. The latter feature is in agreement with present data [5, 7], although within sizeable uncertainties. Improved data and global analyses [11, 12] including checks of the OPE [3] will exhibit whether such effects, which we neglect here, are contributing to $\Delta B = 1$ transitions.

Analytic form factors. For an analytic ansatz for the q^2 -shape of the form factors we employ the Series Expansion (SE) [13–19]. It is based on an expansion in $z(t)$, defined as

$$z(t) \equiv z(t, t_0) = \frac{\sqrt{t_+ - t} - \sqrt{t_+ - t_0}}{\sqrt{t_+ - t} + \sqrt{t_+ - t_0}}, \quad (9)$$

and t being the analytic continuation of q^2 to the complex plane, with $|z| \leq 1$. Here, $t_{\pm} = (m_B \pm m_{K^*})^2$ and $0 \leq t_0 < t_+$ for which we use $t_0 = t_+(1 - \sqrt{1 - t_-/t_+})$ [19, 20].

We define the reduced transversity amplitudes $\hat{f}_i \equiv f_i/\mathcal{N}$, $i = \perp, \parallel, 0$, where the q^2 -dependent normalization factor \mathcal{N} is given in Eq. (6). The SE can then be written as:

$$\hat{f}_i(t) = \frac{(\sqrt{-z(t, 0)})^m (\sqrt{z(t, t_-)})^l}{B(t) \phi_f(t)} \sum_k \alpha_{i,k} z^k(t), \quad (10)$$

with $l = 1, 0, 0$ and $m = 1, 1, 0$ for $i = \perp, \parallel, 0$, respectively. The Blaschke factor $B(t) = z(t, m_R^2)$ parametrizes an off-shell pole associated with a meson with mass m_R ; there can be several such factors if multiple resonances are present. The function $\phi_f(t)$ is given by

$$\phi_f(t) = \sqrt{\frac{\eta}{48\pi\chi_f(n)}} \frac{(t - t_+)}{(t_+ - t_0)^{1/4}} \left(\frac{z(t, 0)}{-t} \right)^{(3+n)/2} \times \left(\frac{z(t, t_0)}{t_0 - t} \right)^{-1/2} \left(\frac{z(t, t_-)}{t_- - t} \right)^{-3/4}, \quad (11)$$

with isospin factor $\eta = 2$, and Wilson coefficients $\chi_f(n)$ with n being the number of subtractions in the renormalization procedure (here $n = 2$), discussed in detail in [19, 20]. We take $\chi_f(2) = 1.2/(100m_b^2)$. Note, that the ratios of the form factors, which are accessible with our analysis, are not sensitive to this input.

	BaBar	CDF		LHCb	
q^2 [GeV ²]	F_L	F_L	$A_T^{(2)}$	F_L	$A_T^{(2)\dagger}$
[14, 18, 16]	$0.43^{+0.13}_{-0.16}$	$0.29^{+0.15}_{-0.14}$	$0.2^{+0.8}_{-0.8}$	$0.35^{+0.10}_{-0.06}$	$0.06^{+0.24}_{-0.29}$
[16, X]	$0.55^{+0.15}_{-0.17}$	$0.20^{+0.20}_{-0.18}$	$-0.7^{+0.9}_{-0.9}$	$0.37^{+0.07}_{-0.08}$	$-0.75^{+0.35}_{-0.20}$

TABLE I: Recent high- q^2 data from BaBar [6], CDF [5] and LHCb [7] with the statistical and systematic uncertainties added in quadrature. The maximum q^2 -value in units of GeV² equals $X = 19$ for LHCb and is the endpoint otherwise.[†] Using $A_T^{(2)} = 2S_3/(1 - F_L)$.

We are constricted to 4 d.o.f., *i.e.*, two bins in the high- q^2 region for each observable, see Table I. Fortunately, we obtain a good fit already for the lowest order SE, where

$$\begin{aligned} f_{\perp}(t) &= \alpha_{\perp} \Lambda(t, m_{1-}^2) \sqrt{-z(t, 0)} \sqrt{z(t, t_-)}, \\ f_{\parallel}(t) &= \alpha_{\parallel} \Lambda(t, m_{1+}^2) \sqrt{-z(t, 0)}, \\ f_0(t) &= \alpha_0 \Lambda(t, m_{1+}^2), \end{aligned} \quad (12)$$

with

$$\Lambda(t, m_R^2) = \frac{\mathcal{N}}{z(t, m_R^2) \phi_T^{V-A}(t)}, \quad \alpha_i \equiv \alpha_{i,0}. \quad (13)$$

We take $m_{1-} = 5.42$ GeV for the vector (\perp) and $m_{1+} = 5.83$ GeV for the axial vector ($\parallel, 0$) transitions [21].

Fit and results. Even though Eqs. (4) is exact for each q^2 , the data on the other hand is binned. In the fit this is taken into account by replacing $f_i^2(q^2)$ with $\int_{\text{bin}} d q^2 (2\rho_1(q^2) f_i^2(q^2))$, where the universal function $\rho_1 = (|C^L|^2 + |C^R|^2)/2$ drops out of Eqs. (4) in the limit of vanishing bin-size. To the accuracy discussed after Eq. (8) we have

$$\rho_1(q^2) = \left| C_9^{\text{eff}}(q^2) + \kappa \frac{2m_b m_B}{q^2} C_7^{\text{eff}}(q^2) \right|^2 + |C_{10}|^2, \quad (14)$$

where $\kappa = 1 - 2\frac{\alpha_s}{3\pi} \ln(\mu/m_b) \simeq 1$, and $C_j^{\text{eff}} = C_j + \dots$ denote the effective coefficients, see [3] for details. Fig. 2 (left-hand plot) shows the slope of ρ_1 in the SM including next-to-leading order QCD corrections as used in the fit (solid curve) and with physics beyond the SM (shaded areas). The latter is estimated by a variation of the Wilson coefficients C_7 from -0.4 to -0.3 and $|C_{10}|$ from 2 to 5, see [12]. Since the bin-averaged shift in the slope is at the percent-level, the uncertainties related to potential contributions from physics beyond the SM are negligible given the current accuracy of the data.

The SE in Eq. (12) is truncated after the first order term, introducing three parameters α_{\perp} , α_{\parallel} and α_0 . Since the data constrains only ratios of the f_i^2 , we are sensitive to the modulus of the ratios of the α_i only. We choose to fit $\alpha_{\parallel}/\alpha_{\perp}$ and α_0/α_{\perp} and obtain $\chi_{\min}^2 = 3.8$ for all data, see Table I. The error correlation of the fit is shown in Fig. 2 (right-hand plot), the fit to the data can be seen in Fig. 1. The best-fit results with 1σ errors are

$$\alpha_{\parallel}/\alpha_{\perp} = 0.43^{+0.11}_{-0.08}, \quad \alpha_0/\alpha_{\perp} = 0.15^{+0.03}_{-0.02} \quad (\text{SE}). \quad (15)$$

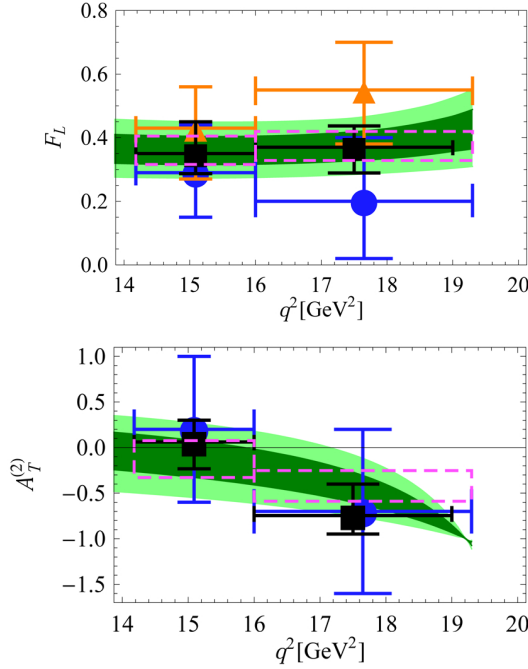


FIG. 1: Experimental data by BaBar [6] (orange triangles), CDF [5] (blue circles) and LHCb [7] (black squares), see Table I, versus the outcome of the fit at 68% CL (dark-green bands unbinned, dashed magenta box binned) 95% CL (light-green bands unbinned) for F_L (top) and $A_T^{(2)}$ (bottom).

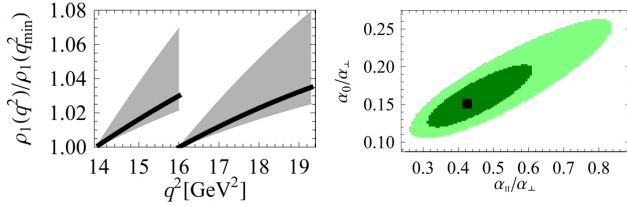


FIG. 2: Left: The function $\rho_1(q^2)$ normalized to its value at $q_{\min}^2 = 14$ and 16 GeV^2 in the SM (solid curve) and with non-SM effects (shaded region). Right: Error correlation of $\alpha_{\parallel}/\alpha_{\perp}$ vs. α_0/α_{\perp} . The shown regions are 68% CL (dark-green), 95% CL (light-green) with the best-fit values given by the black square.

The resulting form factor ratios V/A_1 and A_1/A_2 are presented in Fig. 3. We further show the form factors themselves, fixing $\alpha_{\perp} = -0.08$, *i.e.*, V , to allow for a comparison of the q^2 -shapes. As can be seen, the sensitivity to A_2 is very low towards the endpoint, caused by the λ factor in the transversity amplitude f_0 , see Eq. (5). Also shown are LCSR predictions for $q^2 \lesssim 14$ GeV^2 , where we assigned flat uncertainties as obtained at $q^2 = 0$, *i.e.*, 11%, 12% and 14% for V, A_1 and A_2 , respectively [9]. Quenched [22] (set 3) and unquenched lattice results [2] are shown as well after using the improved Isgur-Wise-relations to lowest order in $1/m_b$ [3, 8]

$$T_1(q^2) = \kappa V(q^2), \quad T_2(q^2) = \kappa A_1(q^2). \quad (16)$$

	SE	SSE	LCSR* [9]	LCSR* [23]
$V(0)/A_1(0)$	2.0 ± 0.4	$3.1^{+0.6}_{-0.7}$	1.4 ± 0.2	1.5 ± 0.9
$A_1(0)/A_2(0)$	1.2 ± 0.1	1.1 ± 0.1	1.1 ± 0.2	1.0 ± 0.7

TABLE II: Form factor ratios at $q^2 = 0$. *Errors symmetrized and added in quadrature.

We add theory uncertainties in quadrature, thereby ignoring possible cancellations of systematics in the ratios. Both lattice and LCSR predictions agree within 95% CL with the ratios obtained from the SE fit.

Using the parametrization of the Simplified Series Expansion (SSE) [18], corresponding to the changes $B(t) \rightarrow 1 - t/m_R^2$, $\phi_f(t) \rightarrow 1$, $\sqrt{-z(t, 0)} \rightarrow \sqrt{t}/m_B$, $\sqrt{z(t, t_-)} \rightarrow \sqrt{\lambda}$ in Eq. (12), a similarly good fit is obtained with $\chi_{\min}^2 = 3.4$ and the best-fit results

$$\alpha_{\parallel}/\alpha_{\perp} = 0.44^{+0.11}_{-0.07}, \quad \alpha_0/\alpha_{\perp} = 0.32^{+0.06}_{-0.04} \quad (\text{SSE}). \quad (17)$$

The form factors from the SSE are in good agreement with the SE ones and not shown. Noticeable differences arise only in the extrapolation to small q^2 , where the SSE results for V/A_1 can be about 50% larger than the ones from SE, however the predictions still overlap within 1σ .

Form factor ratios at $q^2 = 0$ along with LCSR predictions [9, 23] are compiled in Table II. Both fits return values of V/A_1 larger than the LCSR ones and larger than the symmetry-based prediction in the large energy limit $V/A_1 = (m_B + m_{K^*})^2/(m_B^2 + m_{K^*}^2 - q^2)$ [24], *i.e.*, $V(0)/A_1(0) = 1.3$ up to $1/m_b$ corrections [25]. A finer binning is expected to improve the control of the q^2 -shape and the performance of the fit results at low q^2 . We stress, however, that already with present data a consistent picture over the whole physical range is obtained.

Conclusions. Determinations of $B \rightarrow K^*$ form factor ratios from present data and theoretical predictions are mutually consistent, see Fig. 3. The currently still early data may shift towards a larger $A_T^{(2)}$ at low recoil and lead to a correspondingly lower value of V/A_1 , improving the agreement with the preliminary unquenched lattice determination. However, once data have become sufficiently precise allowing for consistency checks [3, 10–12], the low recoil predictions constitute a powerful test for the lattice and its advances [26].

The method of form factor extractions from B -decays into a fully reconstructable final state will greatly benefit in the near-term future from the high-luminosity flavor searches at the LHC; it is applicable to other decays including $\bar{B}_s \rightarrow \phi \mu^+ \mu^-$. Both better statistics and the assessment of further short-distance free observables [3] from a full angular analysis [27] will improve the control of the low recoil region and of the form factors.

Acknowledgments. We are happy to thank Aoife Bharucha, Christoph Bobeth, Danny van Dyk, Stefan Schacht and Matthew Wingate for useful exchanges.

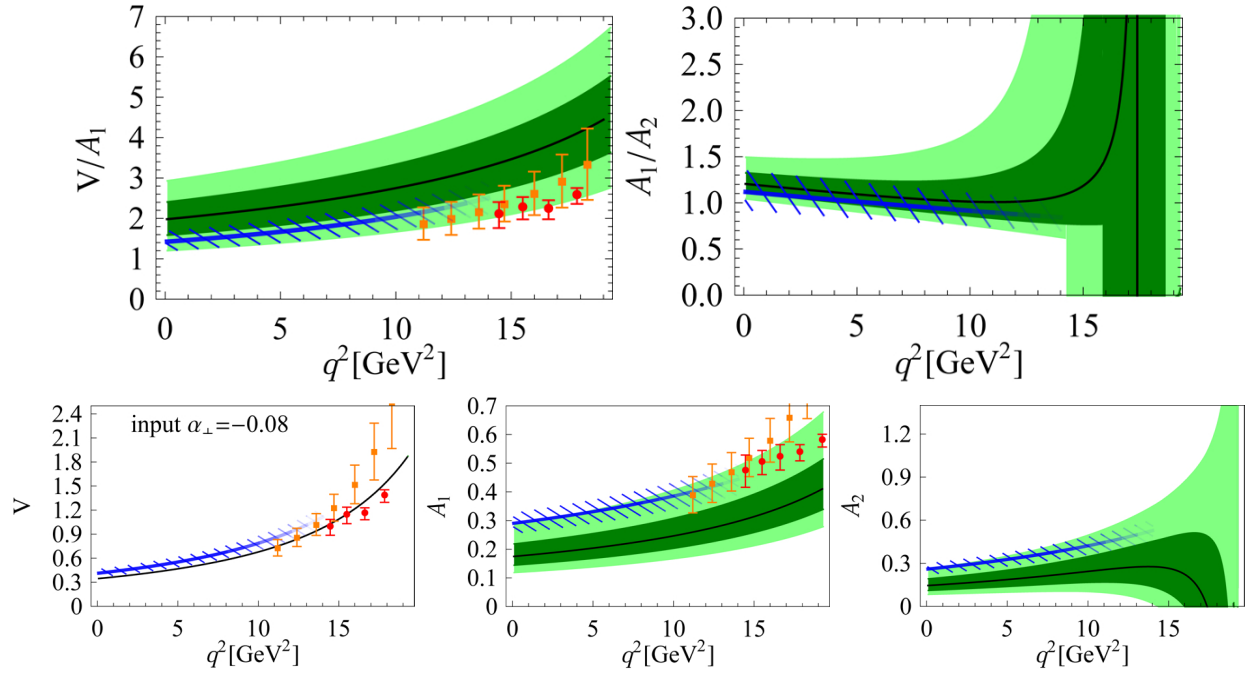


FIG. 3: The form factor ratios V/A_1 and A_1/A_2 from fit to data [5–7] (upper row). In the lower row the form factors are shown using V as input with $\alpha_\perp = -0.08$. The best fit result with 68% CL (95% CL) bands are given by the solid black line and the shaded dark-green (light-green) region, respectively. The solid blue line and the hatched region denote LCSR results [9]. Lattice results from [2] and [22], using the Isgur-Wise relations Eq. (16), are shown as red circles and orange boxes, respectively.

This work is supported in part by the Bundesministerium für Bildung und Forschung (BMBF).

* Electronic address: christian.hambrock@udo.edu

† Electronic address: gudrun.hiller@udo.edu

- [1] P. Ball and V. M. Braun, Phys. Rev. D **58**, 094016 (1998) [hep-ph/9805422].
- [2] Z. Liu *et al.*, arXiv:1101.2726 [hep-ph].
- [3] C. Bobeth, G. Hiller and D. van Dyk, JHEP **1007**, 098 (2010) [arXiv:1006.5013 [hep-ph]].
- [4] F. Kruger and J. Matias, Phys. Rev. D **71**, 094009 (2005) [hep-ph/0502060].
- [5] T. Aaltonen *et al.* [CDF Collaboration], Phys. Rev. Lett. **108**, 081807 (2012) [arXiv:1108.0695 [hep-ex]].
- [6] S. Akar for the BaBar Collaboration at the Lake Louise Winter Institute, Canada, February 23, 2012.
- [7] LHCb Collaboration, CERN-LHCb-CONF-2012-008.
- [8] B. Grinstein and D. Pirjol, Phys. Rev. D **70**, 114005 (2004) [hep-ph/0404250].
- [9] P. Ball and R. Zwicky, Phys. Rev. D **71**, 014029 (2005) [arXiv:hep-ph/0412079].
- [10] M. Beylich, G. Buchalla and T. Feldmann, Eur. Phys. J. C **71**, 1635 (2011) [arXiv:1101.5118 [hep-ph]].
- [11] W. Altmannshofer, P. Paradisi and D. M. Straub, arXiv:1111.1257 [hep-ph].
- [12] C. Bobeth, G. Hiller, D. van Dyk and C. Wacker, JHEP **1201**, 107 (2012) [arXiv:1111.2558 [hep-ph]].
- [13] M. C. Arnesen, B. Grinstein, I. Z. Rothstein and I. W. Stewart, Phys. Rev. Lett. **95**, 071802 (2005) [arXiv:hep-ph/0504209].
- [14] C. G. Boyd, B. Grinstein and R. F. Lebed, Phys. Rev. Lett. **74**, 4603 (1995) [arXiv:hep-ph/9412324].
- [15] C. G. Boyd and M. J. Savage, Phys. Rev. D **56**, 303 (1997) [arXiv:hep-ph/9702300].
- [16] I. Caprini, L. Lellouch and M. Neubert, Nucl. Phys. B **530**, 153 (1998) [arXiv:hep-ph/9712417].
- [17] T. Becher and R. J. Hill, Phys. Lett. B **633**, 61 (2006) [arXiv:hep-ph/0509090].
- [18] C. Bourrely, I. Caprini and L. Lellouch, Phys. Rev. D **79**, 013008 (2009) [Erratum-ibid. D **82**, 099902 (2010)] [arXiv:0807.2722 [hep-ph]].
- [19] A. Bharucha, T. Feldmann and M. Wick, JHEP **1009**, 090 (2010) [arXiv:1004.3249 [hep-ph]].
- [20] R. J. Hill, [arXiv:hep-ph/0606023].
- [21] K. Nakamura *et al.* [Particle Data Group Collaboration], J. Phys. G G **37**, 075021 (2010).
- [22] D. Becirevic, V. Lubicz and F. Mescia, Nucl. Phys. B **769**, 31 (2007) [hep-ph/0611295].
- [23] A. Khodjamirian, T. Mannel, A. Pivovarov and Y. Wang, JHEP **1009**, 089 (2010) [arXiv:1006.4945 [hep-ph]].
- [24] J. Charles *et al.*, Phys. Rev. D **60**, 014001 (1999) [hep-ph/9812358].
- [25] G. Burdman and G. Hiller, Phys. Rev. D **63**, 113008 (2001) [hep-ph/0011266].
- [26] USQCD collaboration, Whitepaper "Lattice QCD and High-Intensity Flavor Physics" November 11, 2011.
- [27] F. Kruger, L. M. Sehgal, N. Sinha and R. Sinha, Phys. Rev. D **61**, 114028 (2000) [Erratum-ibid. D **63**, 019901 (2001)] [hep-ph/9907386].